

# Arsenic and iron speciation and binding in the surface soils in Ningyo-toge mill tailings pond using X-ray absorption fine spectroscopy

Kohei Tokunaga<sup>a,b,\*</sup>, Yoshio Takahashi<sup>c</sup> and Naofumi Kozai<sup>a,b</sup>

<sup>a</sup>Ningyo-toge Environmental Engineering Center, Japan Atomic Energy Agency, Tomata, Okayama 708-0698, Japan

<sup>b</sup>Advanced Science Research Center, Japan Atomic Energy Agency, Tokai, Ibaraki 319-1195, Japan

<sup>c</sup>Department of Earth and Planetary Science, The University of Tokyo, Bunkyo-ku, Tokyo 113-0033, Japan

Received May 12, 2023, Accepted July 11, 2023; Published online July 26, 2023

The mobility of arsenic (As) in the environment is generally controlled by its association with iron minerals through adsorption, coprecipitation, or surface precipitation. In this study, the host phases of As in the surface soil of a mill tailings pond in Ningyo-toge center (Okayama, Japan) were determined using X-ray absorption fine structure (XAFS) spectroscopy. The XAFS analyses showed that (i) Fe is mainly present as Fe(III) (hydr)oxides such as ferrihydrite and goethite, (ii) As occurs as As(V) and may be retained on such (hydr)oxides via adsorption, and (iii) ferrihydrite and goethite are the host phases of As in the surface soil. Although As(V) retention by ferrihydrite in this mill tailings pond has already been reported, this is the first study to demonstrate As(V) retention by goethite in the field.

**Keywords:** arsenic, ferrihydrite, goethite, adsorption, XAFS

## 1. Introduction

The Ningyo-toge uranium (U) mine area, located at the boundary between Okayama and Tottori prefectures in Japan, houses the first U mines to be established in Japan<sup>1</sup>. After the termination of mining activity in 2001, Ningyo-toge Environmental Engineering Center of the Japan Atomic Energy Agency (hereafter, Ningyo-toge center) has managed and maintained the mine sites to prevent environmental contamination. At Ningyo-toge center, groundwater is in contact with U ore-forming minerals (uraninite, ningyoite, coffinite, and autunite) and contaminated with toxic and/or radioactive elements, such as U, radium (Ra), and arsenic (As), via contact with the U ore-forming minerals flows into a mill tailings pond. Since groundwater contains iron (Fe) and manganese (Mn) in the form of Fe(II) and Mn(II) ions, Fe(III) and Mn(IV) (hydr)oxides are formed over the mill tailings pond after the exposure of groundwater to the atmosphere. The concentrations of the aqueous contaminants in the mill tailings pond water are lower than those in the contaminated groundwater and the maximum acceptable concentrations. It is assumed that the (hydr)oxides precipitated in the mill tailings pond remove the contaminants from the contaminated groundwater<sup>2,3</sup>. However, the detailed mechanism of heavy metals retention in the soils in Ningyo-toge mill tailings pond has not been fully understood.

Arsenic, as well as U and Ra, are problematic elements in the Ningyo-toge center. Arsenic is a ubiquitous element found in the atmosphere, soils and rocks, natural and industrial waters, and living organisms<sup>4</sup>. It exists in various oxidation states (-III, 0, III, V) and mostly dissolves in water as arsenite ( $\text{AsO}_2^-$ ) and arsenate ( $\text{AsO}_4^{3-}$ ). The migration of As in the environment has been extensively studied<sup>4–10</sup>. Arsenic often occurs with sulfide and Fe(III) minerals in mill tailings as scorodite ( $\text{FeAsO}_4 \cdot 2\text{H}_2\text{O}$ ) and arsenopyrite ( $\text{FeAsS}$ ), respectively, and is enriched in sediments by adsorption, coprecipita-

tion, or surface precipitation on iron (hydr)oxides<sup>4,7,9</sup>. Arsenic-bearing iron (hydr)oxides, such as ferrihydrite (HFO), goethite ( $\alpha\text{-FeOOH}$ ), and hematite ( $\alpha\text{-Fe}_2\text{O}_3$ ), which play an important role in the retention of As, are typically found in oxidized sediments<sup>4,5,10</sup>.

The purpose of this study is to elucidate the solid phases responsible for As retention and thus, establishes a measure for the safe closure of U mining-related facilities, including the mill tailings pond in Ningyo-toge center. Kawamoto et al. (2021)<sup>2</sup> investigated the speciation of As and Fe in surface soil samples in the field by X-ray absorption near-edge structure (XANES) analysis and found the presence of As and Fe in soils as As(V) and Fe(III), respectively, and that As(V) is preferentially adsorbed on ferrihydrite. However, the previous study lacked information on the local structure of As and Fe in the soils, and the detailed mechanism of As retention is still unknown in term of whether As is adsorbed on ferrihydrite or other iron (hydr)oxides. Therefore, we investigated the local structure of As and Fe in the soil and compared it with synthetic As-adsorbed iron minerals to identify the host phases of As in the natural soils collected in Ningyo-toge mill tailings pond. The extended X-ray absorption fine structure (EXAFS) method was used to determine the binding sites of Fe and As in soils at the field site.

## 2. Materials and methods

**2.1. Ningyo-toge soil samples.** Natural soil and water samples were collected from the mill tailings pond at Ningyo-toge center in Okayama, Japan (Fig. 1a). The sampling site was flooded soil located about 150 m downward from the mine pit (Fig. 1b). Surface soil (0–10 cm) and water were collected using a plastic spatula in November 2022. The pH and redox potential ( $E_h$ ) were measured in situ using a glass electrode (9615S-10D; Horiba, Kyoto, Japan) and an ORP electrode (9300-10D; Horiba), respectively. The measured pH and  $E_h$  values of the surface soil were 5.2 and 482 mV, respectively.

\*Corresponding author. E-mail: tokunaga.kohei@jaea.go.jp

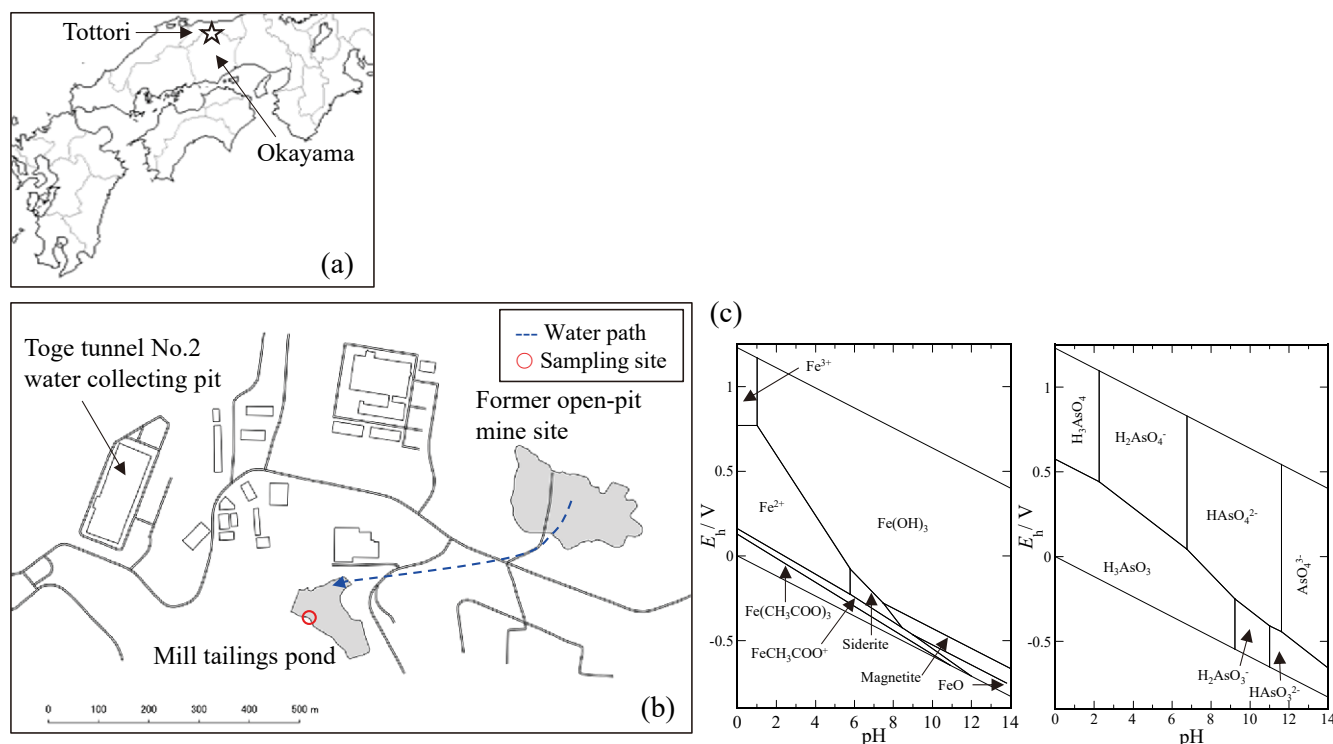


**Figure 1.** (a) Location of U mines around the Ningyo-toge area near the boundary of the Tottori and Okayama prefectures in Japan. (b) Schematic diagram of the Ningyo-toge Environmental Engineering Center of Japan Atomic Energy Agency showing the location of the sampling site. (c)  $E_h$ -pH diagrams of the Fe-CO<sub>2</sub>-H<sub>2</sub>O (Fe =  $1 \times 10^{-3}$  mol L<sup>-1</sup>, pCO<sub>2</sub> 10<sup>-3.5</sup> atoms at 25 °C) and As-H<sub>2</sub>O (As =  $1 \times 10^{-3}$  mol L<sup>-1</sup> at 25 °C) systems showing the equilibrium stability fields for iron phases and arsenic species, plotted with Geochemist's Workbench 12.0 based on the thermodynamic data from GWB, Aqueous Solutions LLC.

To maintain the original chemical composition of the samples before measurements, collected soil samples were dried in a glove box (Coy Laboratory Products Inc., USA) under anaerobic nitrogen conditions (< 10 ppm of O<sub>2</sub>) at room temperature where little transformation of iron minerals, such as ferrihydrite to goethite and hematite or siderite to goethite, occurs. The dried soil samples were then passed through a 500 μm stainless steel sieve to remove large organic particles and gravel fractions, prior to measurements. The homogenized soil samples were packed into polyethylene bags under anaerobic conditions and stored at 4 °C until X-ray absorption fine structure (XAFS) analysis. The water samples were filtered through a mixed cellulose ester membrane filter with a pore size of 0.20 μm (Advantec, Tokyo, Japan). The filtrate was acidified to 2 wt % HNO<sub>3</sub> by adding concentrated HNO<sub>3</sub>.

**2.2. Water and soil analysis.** The As and Fe concentrations in the water samples were measured by inductively coupled plasma mass spectrometry (ICPMS, 7800cs; Agilent, Tokyo, Japan). Concentrations of major elements in the soil were measured by X-ray fluorescence spectrometry (EDX-8100; Shimadzu Corp., Japan). The As concentrations in the soil samples were determined by digesting the samples with HNO<sub>3</sub>/HF fluids under heat treatments, and the filtered solution was analyzed using ICPMS. The mineralogy and morphologies of the samples were studied by X-ray diffraction (XRD, MiniFlex; Rigaku Corp., Japan). The XAFS analysis was also conducted to investigate the speciation and binding sites of As and Fe in the soil.

**2.3 Preparation of the As adsorbed samples.** Two-line ferrihydrite, goethite, hematite, and siderite (FeCO<sub>3</sub>) were selected as iron minerals for XAFS analysis. As shown in Fig. 2, ferrihydrite and goethite were detected in the soil. Hematite was selected as the most common Fe(III) minerals. Siderite was also selected because it was detected by XRD in

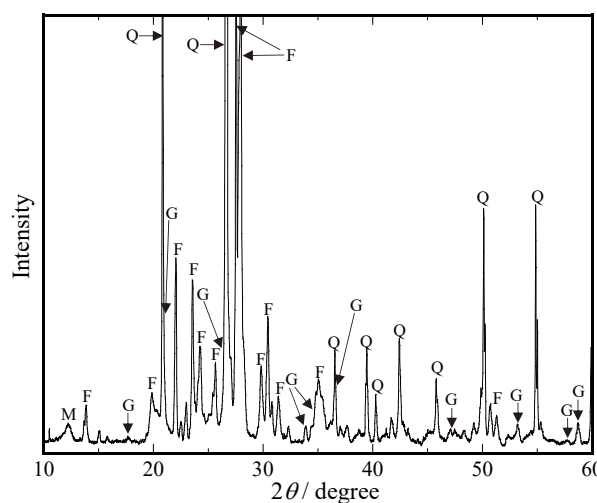


**Figure 2.** X-ray diffraction patterns of the surface soil sample (M, mica; F, feldspar; Q, quartz; G, goethite).

the soil sample collected several meters below the surface (data not shown). Two-line ferrihydrite, goethite, and siderite were synthesized following the method described in previous studies<sup>11,12</sup>. The hematite was purchased from STREM Chemicals Inc. As-adsorbed ferrihydrite, goethite, and hematite samples were prepared by exposing 100 mg of the minerals to KH<sub>2</sub>AsO<sub>4</sub> (Wako, Japan) solution (1 mmol L<sup>-1</sup>, pH 5.0, 50 mL) for 48 h at 25 °C under ambient atmospheric conditions. The solids were collected using a 0.20 μm membrane filter, washed three times with ultrapure water, and stored at 4 °C until XAFS analysis. The mineral phases of the synthesized samples were characterized by XRD with Cu K $\alpha$  radiation at 40 kV voltage and 40 mA current. The solid samples were air-dried under atmospheric and anaerobic conditions before each XRD measurement.

The amount of As adsorbed on the solids ( $C_s$ ,  $\text{mmol kg}^{-1}$ ) and the distribution coefficient ( $K_d$ ,  $\text{L kg}^{-1}$ ) were calculated using the following equations:

$$C_s = |C_i - C_e| \cdot V/m,$$

$$K_d / \text{L kg}^{-1} = C_s / C_e,$$

where  $C_i$  and  $C_e$  are the As concentrations in solution before and after the adsorption ( $\text{mmol L}^{-1}$ ), respectively,  $V$  is the volume of liquid (L), and  $m$  is the weight of solid (kg).

**2.4. XAFS measurement.** Bulk Fe and As K-edge XAFS spectra of the samples were measured at the BL12C of KEK-PF (Ibaraki, Japan) with a Si(111) double-crystal monochromator and two mirrors. The XANES and EXAFS were obtained using the XAFS analyses. The monochromator was calibrated using reference samples, i.e., synthetic goethite and  $\text{KAsO}_2$  (Wako, Japan), which was prepared as a pellet after dilution with boron nitride powder. The energy values of 7.111 and 11.865 keV were assigned to the pre-edge and main-edge peaks in the XANES region of the compounds of Fe and As, respectively. XAFS spectra of the reference samples were collected in transmission mode, while those of the experimental samples were obtained in the fluorescence mode using a 19-element germanium semiconductor detector placed at  $90^\circ$  to the incident beam.

The EXAFS spectra were analyzed by normal procedures using REX2000 software (Rigaku Co. Ltd.) with the parameters generated by the FEFF 7.0 code. Following background subtraction and normalization, EXAFS oscillations  $k^3 \chi(k)$  were extracted from the raw data. After extracting EXAFS oscillations and their Fourier transformations, the inversely Fourier filtered data were analyzed using a conventional curve fitting method.

XANES linear combination fitting (LCF) was performed to quantify the relative abundance of Fe and As species in the soils. Solid-phase Fe and As speciation was further evaluated by fitting of  $k^3$  weighted EXAFS spectra of soil samples against corresponding spectra from references using the Athena interface to IFEFFIT<sup>13</sup>. The goodness of fit param-

eters used for LCF are  $R$ -factor, which is defined by

$$R \text{ factor} = \Sigma (\text{data} - \text{fit})^2 / \Sigma \text{data}^2$$

where the low  $R$ -factor represents a better match between the standard spectra and the sample spectrum.

### 3. Results and discussion

**3.1. Soil and water characterization.** The properties of the soil samples were summarized in Table 1. The soil contained high levels of Si (57.1 wt.%), Fe (17.7 wt.%), and Al (15.7 wt.%). The As concentration of the soil ( $1.1 \times 10^3 \text{ mg kg}^{-1}$ ) was about five orders of magnitude higher than that of the water ( $2.3 \times 10^{-2} \text{ mg L}^{-1}$ ), indicating that the As in the water flowing into the mill tailings pond was enriched in the surface soil. Arsenic-bearing minerals, such as scorodite and

**TABLE 1: Chemical composition of the surface soil and water in Ningyo-toge mill tailings pond.**

Element	Soil / %	Pond water
Si	57.1	-
Fe	17.7	-
Al	15.7	-
Ca	4.0	-
Ti	2.7	-
Na	1.5	-
S	0.31	-
P	0.24	-
Cu	0.22	-
Sr	0.20	-
Mn	0.10	-
Total	99.8	-
	$\text{mg kg}^{-1}$	$\text{mg L}^{-1}$
As	$1.1 \times 10^3$	$2.3 \times 10^{-2}$
Fe	$1.6 \times 10^5$	$1.7 \times 10^0$

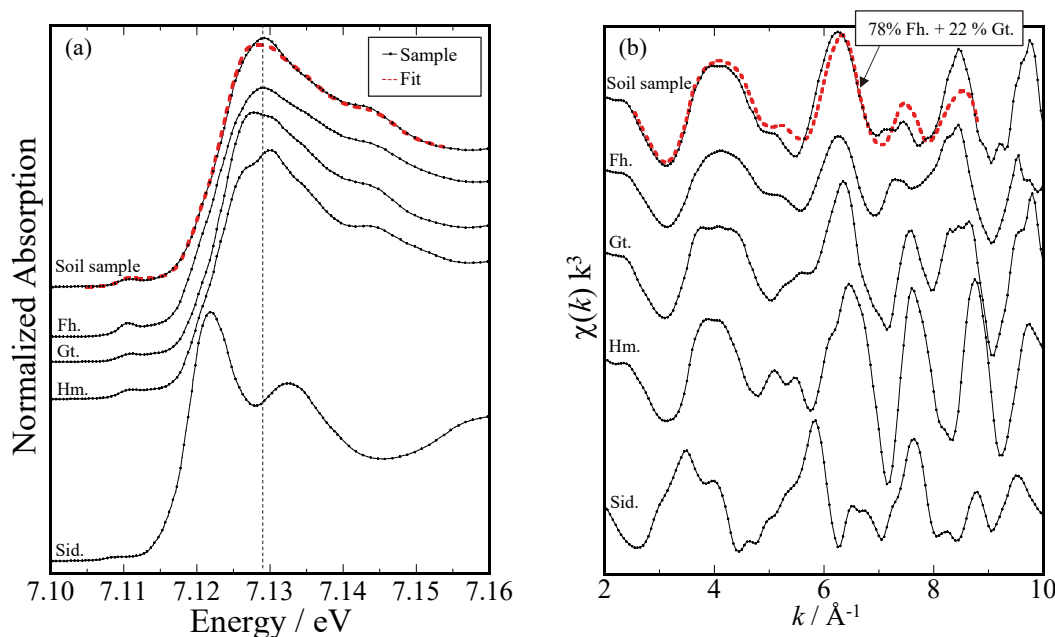


**Figure 3.** (a) Fe K-edge XANES spectra of the soil sample and references. Two Line-ferrihydrite, goethite, hematite, and siderite are present as Fh., Gt., Hm., and Sid., respectively. The black broken lines indicate the binding energy of the main peak of two-line-ferrihydrite. (b) Fe K-edge EXAFS spectra of the soil sample and references.

arsenopyrite, were not observed in the XRD spectrum of the soil (Fig. 2). The major crystalline minerals in the soil were quartz, albite, mica, and goethite. Although Fe was enriched in the soil, goethite was a minor component, and other iron minerals were not observed in the XRD patterns. Such Fe enrichment may have been due to the presence of ferrihydrite in the soil, which is not detected by XRD analysis because of its amorphous structure.

The formation of iron phases and aqueous As species can be estimated from pH- $E_h$  diagrams. Considering the pH (5.2) and  $E_h$  (482 mV) values recorded at the site (Fig. 1), iron (hydr) oxides such as ferrihydrite, goethite, and hematite are the predicted stable phase and As occurs as As(V) ( $H_2AsO_4^-$ ) in aqueous solution.

**3.2. XAFS Analyses for Fe and As.** The Fe species in the soil samples were characterized by XAFS at the Fe K-edge. The features around the absorption edge of the sample are similar to those of ferrihydrite and differ from those of the other Fe minerals (Fig. 3a). The fraction of the Fe phases was determined by the LCF analysis of the  $k^3$  weighted EXAFS oscillations (in the 2.5–8.8  $\text{\AA}^{-1}$  range) of the samples against corresponding spectra from references including ferrihydrite, goethite, hematite, and siderite (Fig. 3b). The amplitude of the  $k^3 \chi(k)$  function at  $k$  around 5–6  $\text{\AA}^{-1}$  clearly differs in all references, and the Fe fractions of the soil sample are estimated to be ferrihydrite (78%) and goethite (22%) ( $R=0.09$ ). These results indicate that the major oxidation state of Fe is Fe(III), and Fe is mainly present as Fe(III) (hydr)oxides such as ferrihydrite and goethite in the surface soil.

Figure 4a shows the As K-edge XANES spectra for references and the soil sample. The XANES spectrum of the sample was very similar to that of  $KH_2AsO_4$ , suggesting that As exists as As(V) in the soil. This is in agreement with the main chemical species of As in water ( $H_2AsO_4^-$ , As(V)) estimated from the pH and  $E_h$  values at the site (Fig. 1c).

The local structure of As was examined by EXAFS to obtain information on the host phases of As(V) in the soil. As reference samples, the As(V)-adsorbed ferrihydrite, goethite,

hematite, and siderite samples were investigated by EXAFS. The  $K_d$  values of As for these iron minerals determined by the adsorption experiments are summarized in Table 2. The Fourier transformation of EXAFS spectra (figure not shown) is consistent with previous EXAFS studies for As(V) on ferrihydrite<sup>14,15</sup>, goethite<sup>14-16</sup>, hematite<sup>14</sup>, and siderite<sup>14,15</sup>. The As K-edge  $k^3$  weighted EXAFS spectra of the soil sample and references are shown in Fig. 4b.

According to the LCF of the  $k^3$  weighted EXAFS spectra (in the 2.8–11.5  $\text{\AA}^{-1}$  range), the As fractions of each binding site in the sample are estimated to be As(V)-adsorbed ferrihydrite (70%) and As(V)-adsorbed goethite (30%), in accordance with the LCF results of Fe K-edge XAFS spectra. Figure 4(c) shows the comparison of LCF results obtained from (i) As(V)-adsorbed ferrihydrite (70%) and As(V)-adsorbed goethite (30%) ( $R=0.08$ ), (ii) As(V)-adsorbed goethite ( $R=0.20$ ), and (iii) As(V)-adsorbed ferrihydrite ( $R=0.12$ ). The best fits of the sample are obtained from (i), as indicated by the low R factor, due to the specific features of EXAFS oscillations of the sample at  $k$  around 4.8 and 7.2  $\text{\AA}^{-1}$ . These results indicate that both ferrihydrite and goethite are the host phase of As in the surface soil and that the As flowing into the Ningyo-toge mill tailings pond is removed from the water mainly by adsorption. This is the first study to demonstrate the occurrence of As(V)-adsorbed goethite in Ningyo-Toge mill tailings pond.

**3.3. As mobility in Ningyo-toge mill tailings pond.** This study showed that the soil As(V) samples are associated with iron (hydr)oxides that have high adsorption capacity and affinity for heavy metals, including As. However, the cause for adsorption of As(V) on both ferrihydrite and goethite remains unclear. Previous studies have shown that goethite has a low adsorption capacity for As(V) compared with ferrihydrite<sup>4,17,18</sup>. This study also revealed that the  $K_d$  value for goethite was approximately three orders of magnitude lower than that for ferrihydrite (Table 2). However, the XAFS results showed the occurrence of As(V)-adsorbed ferrihydrite (70%) and As(V)-adsorbed goethite (30%) in the mill tailings pond, which is in consistent with the adsorption capacity of the iron (hydr)

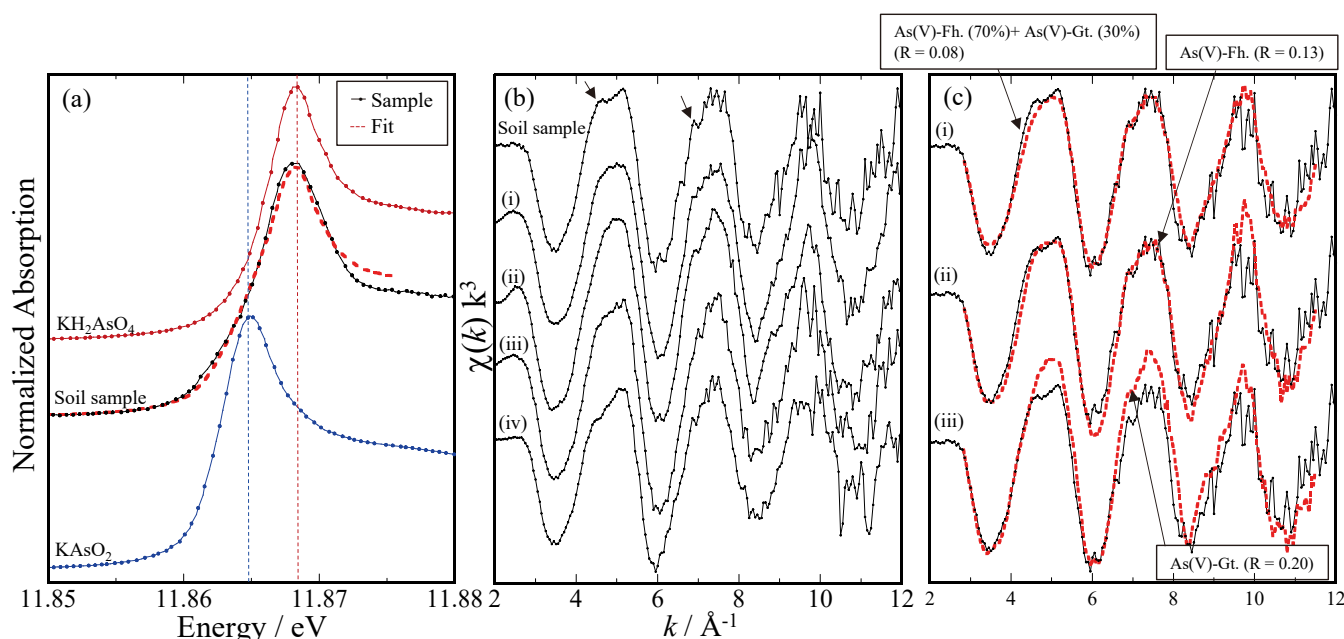


**Figure 4.** (a) As K-edge XANES spectra of soil sample and references. The red broken lines indicate the binding energy of main peak of  $KH_2AsO_4$ , respectively. The blue broken line indicates the binding energy of main peak of  $KAsO_2$ . (b) As K-edge EXAFS spectra of the soil sample and As(V)-adsorbed samples. As(V)-adsorbed samples of (i) As(V)-adsorbed Fh., (ii) As(V)-adsorbed Gt., (iii) As(V)-adsorbed Hm., and (iv) As(V)-adsorbed Sid. (c) Experimental spectra of the soil sample and calculated fits using linear combination fitting (LCF) obtained from (i) As(V)-adsorbed ferrihydrite (70%) and As(V)-adsorbed goethite (30%) ( $R=0.08$ ), (ii) As(V)-adsorbed ferrihydrite ( $R=0.13$ ), and (iii) As(V)-adsorbed goethite ( $R=0.20$ ).



TABLE 2: Adsorption capacity of As(V) for iron minerals.

Samples	$C_i$ / mmol L <sup>-1</sup>	$C_e$ / mmol L <sup>-1</sup>	$Q_s$ / mmol kg <sup>-1</sup>	$K_d$ / L kg <sup>-1</sup>
2 Line ferrihydrite (oxic)	$1.3 \times 10^0$	$2.0(\pm 0.2) \times 10^{-2}$	$6.2(\pm 0.0) \times 10^2$	$3.2(\pm 0.2) \times 10^4$
Goethite (oxic)	$1.3 \times 10^0$	$8.9(\pm 0.2) \times 10^{-1}$	$1.9(\pm 0.1) \times 10^2$	$2.1(\pm 0.1) \times 10^2$
Hematite (oxic)	$1.1 \times 10^0$	$1.0(\pm 0.2) \times 10^0$	$3.5(\pm 1.0) \times 10^1$	$3.5(\pm 1.0) \times 10^1$
Siderite (anoxic)	$1.3 \times 10^0$	$1.2(\pm 0.0) \times 10^{-2}$	$5.9(\pm 0.0) \times 10^2$	$4.9(\pm 0.0) \times 10^4$

oxides under experimental conditions. Previous studies have also shown that As(V)-adsorbed ferrihydrite transforms to goethite and hematite with time<sup>10,19,20</sup>, and a large amount of As(V) is believed to be released into solution and doesn't remain adsorbed on the goethite surface during the transformation<sup>5,19,21-23</sup>. Therefore, it is considered that As(V)-adsorbed goethite in the field site is not formed by the simple adsorption of As(V) on goethite and transformation of As(V)-adsorbed ferrihydrite to goethite.

The enrichment of As(V) in goethite may be due to several factors, such as abiotic and biotic features of the environment. We considered (i) the interaction of organic matter with mineral surfaces<sup>24</sup> and (ii) the transformation of other iron minerals (e.g., siderite<sup>12,25,26</sup> and schwertmannite<sup>27,28</sup>) to goethite. For example, one hypothesis is based on the transformation of siderite, which is detected in the several meters below the surface (data not shown), to goethite. Previous studies have shown that the transformation of siderite to goethite from anoxic to oxic conditions increases the adsorption capacity of As(V) on goethite by an order of magnitude<sup>12,25</sup>. Thus, it is considered that siderite precipitated in deep soils under anoxic conditions transforms to goethite in surface soils under oxic conditions, and then the enrichment of As(V) in goethite occurs during the transformation. This is a hypothesis and the details of the As retention behavior in the field remain unknown, and will be a topic of our future research.

#### 4. Conclusions

This study revealed that both ferrihydrite and goethite are the host phases of As in the surface soils in Ningyo-toge mill tailings pond. To the best of our knowledge, this is the first study to investigate the local structure of Fe and As in soils collected in the mill tailings pond by EXAFS analysis. The novelty of this study is that some of the As can be stabilized by adsorption on goethite and occurs as As(V)-adsorbed goethite in the surface soils. These results indicate that As flowing into the Ningyo-toge mill tailings pond is removed from water mainly by adsorption on ferrihydrite and goethite in the field. These findings would help remediate contaminated soils and predict the long-term behavior of As in the natural environment.

#### Acknowledgements

This work was carried out under the approval of the Photon Factory (nos. 2021G076 and 2022G512). Financial support was partly provided by JSPS KAKENHI Grant Number JP 23K13693 and by ERAN Y-23-04. This study was also partly performed under the subsidy program "Project of Decommissioning, Contaminated Water and Treated Water Management (Research and Development of Processing and Disposal of Solid Waste)" conducted by the Ministry of Economy, Trade and Industry of Japan.

#### References

[1] Muto T, Meyrowitz R, Pommer AM, Murano T (1959)

- Ningyoite, a new uranous phosphate mineral from Japan. *American Mineralogist: Journal of Earth and Planetary Materials*, 44(5-6): 633–650.
- [2] Kawamoto K, Yokoo H, Ochiai A, Nakano Y, Takeda A, Oki T, Takehara M, Uehara M, Fukuyama K, Ohara Y, Ohnuki T, Hochella MF, Utsunomiya S (2021) The role of nanoscale aggregation of ferrihydrite and amorphous silica in the natural attenuation of contaminant metals at mill tailings sites. *Geochim Cosmochim Acta*, 298: 207–226.
- [3] Takeda A, Oki T, Yokoo H, Kawamoto K, Nakano Y, Ochiai A, Winarni ID, Kitahara M, Miyoshi K, Fukuyama K, Ohara Y, Yamaji K, Ohnuki T, Hochella MF, Utsunomiya S (2023) Direct observation of Mn distribution/speciation within and surrounding a basidiomycete fungus in the production of Mn-oxides important in toxic element containment. *Chemosphere*, 313: 137526.
- [4] Smedley PL, Kinniburgh DG (2002) A review of the source, behaviour and distribution of arsenic in natural waters. *Applied geochemistry*, 17(5): 517–568.
- [5] Majzlan J, Lalinská B, Chovan M, Jurkovič LU, Milovská S, Göttlicher J (2007) The formation, structure, and ageing of As-rich hydrous ferric oxide at the abandoned Sb deposit Pezinok (Slovakia). *Geochim Cosmochim Acta*, 71(17): 4206–4220.
- [6] Mitsunobu S, Harada T, Takahashi Y (2006) Comparison of antimony behavior with that of arsenic under various soil redox conditions. *Environ Sci Technol*, 40(23): 7270–7276.
- [7] Yamaguchi N, Nakamura T, Dong D, Takahashi Y, Amachi S, Makino T (2011) Arsenic release from flooded paddy soils is influenced by speciation, Eh, pH, and iron dissolution. *Chemosphere*, 83(7): 925–932.
- [8] Tokunaga, K, Uruga, T, Nitta, K, Terada, Y, Sekizawa, O, Kawagucci, S, Takahashi, Y (2016) Application of arsenic in barite as a redox indicator for suboxic/anoxic redox condition. *Chem Geol*, 447: 59–69.
- [9] Itabashi T, Li J, Hashimoto Y, Ueshima M, Sakanakura H, Yasutaka T, Imoto Y, Hosomi, M (2019) Speciation and fractionation of soil arsenic from natural and anthropogenic sources: chemical extraction, scanning electron microscopy, and micro-XRF/XAFS investigation. *Environ Sci Technol*, 53(24): 14186–14193.
- [10] Shi M, Min X, Ke Y, Lin Z, Yang Z, Wang S, Wei Y (2021) Recent progress in understanding the mechanism of heavy metals retention by iron (oxyhydr) oxides. *Sci Total Environ*, 752: 141930.
- [11] Cornell RM, Schwertmann U (2003) *The iron oxides: structure, properties, reactions, occurrences, and uses* (Vol. 664). Weinheim, Germany.
- [12] Guo H, Ren Y, Liu Q, Zhao K, Li Y (2013) Enhancement of arsenic adsorption during mineral transformation from siderite to goethite: mechanism and application. *Environ Sci Technol*, 47(2): 1009–1016.
- [13] Newville M (2001) EXAFS analysis using FEFF and FEFFIT. *Journal of synchrotron radiation*, 8(2): 96–100.
- [14] Sherman D M, Randall S R (2003) Surface complexation of arsenic (V) to iron (III)(hydr) oxides: structural mech-

- anism from ab initio molecular geometries and EXAFS spectroscopy. *Geochim Cosmochim Acta*, 67(22), 4223–4230.
- [15] Yang S, Uesugi S, Qin H, Tanaka M, Kurisu M, Miyamoto C, Kashiwabara T, Usui A, Takahashi Y (2018) Comparison of arsenate and molybdate speciation in hydrogenetic ferromanganese nodules. *ACS Earth and Space Chemistry*, 3(1): 29–38.
- [16] Jönsson J, Sherman DM (2008) Sorption of As (III) and As (V) to siderite, green rust (fougerite) and magnetite: Implications for arsenic release in anoxic groundwaters. *Chemical Geology*, 255(1-2): 173–181.
- [17] Ona-Nguema G, Morin G, Juillot F, Calas G, Brown GE (2005) EXAFS analysis of arsenite adsorption onto two-line ferrihydrite, hematite, goethite, and lepidocrocite. *Environ Sci Technol*, 39(23): 9147–9155.
- [18] Jiang X, Peng C, Fu D, Chen Z, Shen L, Li Q, Ouyang T, Wang Y (2015) Removal of arsenate by ferrihydrite via surface complexation and surface precipitation. *Applied Surface Science*, 353: 1087–1094.
- [19] Waychunas GA, Rea BA, Fuller CC, Davis JA (1993) Surface chemistry of ferrihydrite: Part 1. EXAFS studies of the geometry of coprecipitated and adsorbed arsenate. *Geochim Cosmochim Acta*, 57(10): 2251–2269.
- [20] Catalano JG, Luo Y, Otemuyiwa B (2011) Effect of aqueous Fe (II) on arsenate sorption on goethite and hematite. *Environ Sci Technol*, 45(20): 8826–8833.
- [21] Ford RG (2002) Rates of hydrous ferric oxide crystallization and the influence on coprecipitated arsenate. *Environ Sci Technol*, 36(11): 2459–2463.
- [22] Erbs JJ, Berquó TS, Reinsch BC, Lowry GV, Banerjee SK, Penn RL (2010) Reductive dissolution of arsenic-bearing ferrihydrite. *Geochim. Cosmochim. Acta*, 74(12): 3382–3395.
- [23] Mitsunobu S, Muramatsu C, Watanabe K, Sakata M (2013) Behavior of antimony (V) during the transformation of ferrihydrite and its environmental implications. *Environ Sci Technol*, 47(17): 9660–9667.
- [24] Shu Z, Pan Z, Wang X, He H, Yan S, Zhu X, Song W, Wang, Z (2022) Sunlight-Induced Interfacial Electron Transfer of Ferrihydrite under Oxidic Conditions: Mineral Transformation and Redox Active Species Production. *Environ Sci Technol*, 56(19): 14188–14197.
- [25] Guo H, Li Y, Zhao K (2010) Arsenate removal from aqueous solution using synthetic siderite. *Journal of hazardous materials*, 176(1–3): 174–180.
- [26] Stolze L, Zhang D, Guo H, Rolle M (2019) Model-based interpretation of groundwater arsenic mobility during in situ reductive transformation of ferrihydrite. *Environ Sci Technol*, 53(12): 6845–6854.
- [27] Burton ED, Bush RT, Sullivan LA, Mitchell DR (2008) Schwertmannite transformation to goethite via the Fe (II) pathway: Reaction rates and implications for iron–sulfide formation. *Geochim Cosmochim Acta*, 72(18): 4551–4564.
- [28] Burton ED, Johnston SG, Kraal P, Bush RT, Claff S (2013) Sulfate availability drives divergent evolution of arsenic speciation during microbially mediated reductive transformation of schwertmannite. *Environ Sci Technol*, 47(5): 2221–2229.